Online ISSN 1848-3380, Print ISSN 0005-1144
ATKAFF 57(4), 936–947(2016)

Petar J. Mišljen, Željko V. Despotović, Milan S. Matijević

Modeling and Control of Bulk Material Flow on the Electromagnetic Vibratory Feeder

DOI 10.7305/automatika.2017.03.1766
UDK 681.532.015.017:636.084.7-868-523.2

Original scientific paper

This paper presents the results of modeling, simulation and experimental research of the bulk material flow on the electromagnetic vibratory feeder (EVF). The model of the EVF was implemented in Simulink/Matlab and verified in the experimental research. It has been experimentally confirmed that the bulk material flow rate has its maximal value as far as excitation frequency is equal to the EVF mechanical resonant frequency. For certain bulk material flow rate, average value of excitation coil current of EVF has minimal value when named frequencies are equal. In addition to modeling of the EVF, the main contribution of this paper is implementation of flow control algorithm of bulk material on EVF, experimental verification of the adopted model and defines parameters that enable the selection of energy-efficient operating point of the EVF.

Key words: Actuator, Power Converter, Electromagnetic excitation, Frequency, PWM, Vibratory feeder, Flow control

Modeliranje i upravljanje tokom rasutog materijala na elektromagnetskoj vibrirajućoj hranilici. U ovom radu su predstavljeni rezultati modeliranja, simulacije i eksperimentalnog istraživanja toka rasutog materijala na elektromagnetskoj vibrirajućoj hranilici (EVF). Model EVF-a je implementiran u Simulinku/Matlabu i eksperimentalno provjeren. Eksperimentalno je potvrđeno da brzina toka rasutog materijala ima maksimalnu vrijednost dok je uzbudna frekvencija jednaka mehaničkoj rezonantnoj frekvenciji EVF-a. Za određene brzine tokova rasutog materijala, srednja vrijednost uzbudne struje zavojnice EVF-a ima minimalnu vrijednost u trenutku kada su nazivne frekvencije jednake. Uz model EVF-a glavni doprinosi ovog rada su implementacija algoritma za upravljanje tokom rasutog materijala na EVF-u, eksperimentalna potvrda razvijenog modela i definiranje parametara koji omogućuju izbor energetski efikasne radne točke EVF-a.

Ključne riječi: Aktuator, Energetski pretvarač, Elektromagnetska pobuda, Frekvencija, PWM, Vibracijska hranilica, Upravljanje tokom

1 INTRODUCTION

Vibratory feeders with electromagnetic excitation are used in the industry of bulk and particulate materials processing (conveying, dosing, screening, etc.). The essential parts of the typical electromagnetic vibratory feeder (EVF) are: foundation with supporting base, elastic mounted horizontal or inclined trough for conveying of bulk or particulate material and electromechanical driving device i.e. electromagnetic vibratory actuator (EVA). The material is placed on the vibratory through. The principle of the material conveying is based on the micro-throw or sliding of material particle, depending on the value of the vertical component of vibratory acceleration acting on the particles [1-4].

The conveying rate of material is determinated by the excitation frequency and vibratory width (double vibratory amplitude) of vibrating trough. The excitation frequency is in the frequency range 5 Hz - 150 Hz and vibratory width is in the range 0.1 mm – 20 mm, for most of particulate and granular materials [1], [5-6].

A very important component in the EVF is the EVA. By its essence, the EVA is usually represented as an electromagnetic generator of mechanical force. This mechanical force is proportional to the square of the EVA current. If the excitation current (i.e. EVA current) has pulsed nature, then the corresponding electromagnetic force will also be pulsed. Application of electromagnetic vibratory drive in combination with switching power converter provides flexibility during operation. In other words, in this way it is possible to adjust the frequency of driving electromagnetic forces, as well as its duration and amplitude. In this way, the whole conveying system with EVF has a behavior of the controllable mechanical oscillator [7-12].

On the other hand electromagnetic drives offer easy

and simple control of the gravimetric flow of conveying materials. In comparison to all other mechanical drive actuators (inertial, eccentric, centrifugal, etc.), electromagnetic drives have a simpler construction and they are compact, robust and reliable in operation. The absence of mechanical part wear, such as with gears, cams belts, bearings, eccentrics or motors, makes electromagnetic vibratory conveyors and EVF most economical equipment [10-12]. The elastic elements of EVF are made from composite leaf springs which are subject to very high dynamic strain and they are the most critical element of the vibratory conveying device from the standpoint of safety and reliability [13-15].

From the standpoint of energy efficiency in industrial applications resonant EVF drives are of particular interest. The selection of stiffness of composite leaf springs for the predefined mass of conveying material, affects the mechanical resonant frequency. Operation in the mechanical resonance is favourable from the energy point of view, since it requires minimal energy consumption. In this case finite, but limiting values of the oscillation amplitude can be obtained for relatively small energy of excitation. The limitation of amplitude oscillations is provided by adequate amplitude control, while the searching and tracking of resonant frequency are provided by adequate frequency control. So, this concept implies the using the regulated EVF drives in which implement amplitude-frequency control. Regulated resonant EVF drive additionally provides the highest energy efficiency: minimum value of EVA coil current, minimum EVA coil heating, minimum power consumption [7-9] and improves input power factor of whole regulated EVF drive [16].

The study [7] showed that the sensitivity of the EVF to disturbances in the form of rapid change of the mass of transferred bulk material can be significantly reduced by introducing feedback and use of proportional-integral (PI) controller. In the particular application, the considered thyristor (i.e. SCR) drive is with amplitude control and there is no possibility of adjusting the frequency. The operating frequency is fixed on the value of 50Hz.

References [10], [12] discuss the structures of high performance feedback controllers for EVF. The EVA is driven by the switching circuit with pulse width as control variable. The controller structure consists of a PI controller combined with the state observer. The controlled variables are the resonant frequency and vibration amplitude obtained in real time from the state observer. Use of the state observer allows fast disturbance rejection and reference tracking in both directions (amplitude increase and decrease).

Although references [7], [10] and [12] provide a comprehensive and significant practical and scientific contribution, they do not treat the problem of bulk material flow. Therefore, in this paper we have tried to clarify certain issues, particularly those related to the dynamics of the bulk material which is transported along the vibrating trough of EVF.

The main contribution of this paper is to determine the impact of the frequency and average value of EVA coil current (i.e. frequency of excitation force) of the EVF on the bulk material flow rate.

For this reason a comprehensive Matlab/Simulink model of the EVF system has been developed including the bulk material conveyance model, and simulation results are compared with those obtained on the experimentally realized laboratory setup. Achievement of this investigation contributes to future research of the EVF.

An experimental setup has been designed for research of the bulk material flow on the EVF. Based on the model of digital control unit, the mathematical model of the EVF and the approximate mathematical model of the relative movement of bulk material in relation to the vibrating trough, has been implemented along with the EVF model in Simulink/Matlab. This model represents an additional and significant contribution to the scientific study of the EVF.

For the purpose of recording frequency characteristics of the EVF, the springs had been changed so that the frequency characteristics were recorded for three cases of EVF mechanical resonant frequencies. The bulk material flow rate and the average value of EVA coil current of the EVF have been measured for many different values of the coil current frequency, in order to provide experimental verification of the adopted EVF model.

The additional significance of the proposed work relates to the fact that the vibration problem is also present in many other areas and it is the subject of various studies. One example is the technology of repairing the disc chipper and the balancing process of the disc chipper in its own bearings [18].

2 MATHEMATICAL MODEL OF VIBRATORY FEEDER LOADED WITH TRANSPORTING MATERIAL

Block diagram of the mathematical model of EVF is presented in Fig. 1.

Input parameters $M_1\,[kg]$, $A\,[\%]$ and $f\,[Hz]$ represent mass of material that flow from inlet hopper during one period of mechanical oscillation, excitation power parameter and excitation frequency of the solenoid, respectively. Excitation power parameter ($A\,[\%]$) is a parameter that represents the percentage of maximum power which could be forwarded to the solenoid coil and it is proportional to the average value of the coil current ($I_c\,[mA]$). The control

unit controls the operation of the energy converter that generates a PWM voltage waveform. Variable p represents a displacement of the moving armature core in a horizontal plane.

The power converter is asymmetrical half-bridge and operates on the principle of PWM. A typical waveform and schematic diagram of the power converter are shown in Fig. 2 and Fig. 3.

In the above case, triangular signals (signal 1 and signal 4) are used as reference signal and carrier signal, respectively. By comparing these two signals the corresponding PWM signal is obtained which controls the operation of the switch Q1 and Q2. These two switches are driving simultaneously. While these switches are closed, the voltage of EVA is equal +Vs, and consequently the EVA coil current (*i*) increases. With the opening of the switches, diodes D1 and D2 become conductive, the voltage on the EVA coil is equal –Vs and consequently decreasing of EVA coil current. The EVA coil current signal is presented by the *signal 2*.

Mechanical part of the EVF, including EVA can be mathematically presented by the differential equations [12].

The second-order model of the mechanical part is used here

$$\ddot{p} + 2\varsigma\omega_0 \dot{p} + \omega_0^2 (p - p_0) = K_p \omega_0^2 f_c \tag{1}$$

where p, ς, ω_0, p_0, K_p and f_c denote the measured displacement of trough with respect to the unmoving support, the damping factor, the resonant frequency, the equilibrium position of trough, the static gain, and the force, respectively. Mechanical force f_c is produced by the electromagnet.

Detailed model of EVA, presented in [12], can be represented in the form:

$$L(p) \cdot \frac{di_c}{dt} + \left(\frac{\partial L(p)}{\partial p} \cdot \frac{dp}{dt} + R_c \right) \cdot i_c = u \tag{2}$$

$$f_c = \frac{1}{2} \cdot \frac{\partial L(p)}{\partial p} \cdot i_c^2 \tag{3}$$

where R_c represents active resistance and $L(p)$ inductance of EVA coil:

$$L(p) = L_0 \cdot \frac{p_0}{d + p} \tag{4}$$

The dependence of the coil inductance with respect to the air-gap width is shown on the Fig. 4. Inductance values shown in the figure, are obtained by experimental measurements.

Quantities i_c, u and L_0 represent EVA current, EVA voltage and inductance of EVA coil when the armature is passing through the equilibrium position, i.e. when$p = p_0$, respectively. The bronze disk with sufficient thickness doesn't permit inductor to form a complete magnetic circuit between moving core and stator iron; in other words, it inhibits "gluing" of armature and inductor, which is undesirable. In practical cases $d << p_0$ needs to be satisfied.

The ***envelope detector*** is an electronic circuit that takes a high-frequency signal as input and provides an output which is the envelope of the original signal. The simplest form of envelope detector is the diode detector, i.e. a diode between the input and output of a circuit, connected to a resistor and capacitor in parallel from the output of the circuit to the ground. The capacitor in the circuit stores up charge on the rising edge, and releases it slowly through the resistor when the signal falls. The diode in series rectifies the incoming signal, allowing current flow only when the positive input terminal is at a higher potential than the negative input terminal. If the resistor and capacitor are correctly chosen, the output of this circuit should approximate a voltage-shifted version of the original signal. A simple filter can then be applied to filter out the DC component. In this case, the output from the envelope detector is the amplitude of oscillation of the solenoid plunger (P).

Based on the value of the parameter P, the velocity of the material flowing through the vibrating trough is calculated. The model of the relative movement of bulk material in relation to the vibrating trough is shown in [17]. Principal diagram of the linear vibratory conveyor including its external driving is shown in Fig. 5. Mechanical force f_c from (1) is horizontal component of the resulting excitation forces which act on the trough.

The transition from sliding to hopping happens as soon as the condition $\omega^2 P tg\alpha \sin \omega t - g > 0$, with g being the gravitational constant, is fulfilled.

During sliding phase the corresponding equation of motion is determined by

$$\ddot{x} + \mu_F \dot{x} = \omega^2 P_a \sin \omega t - \mu sgn(\dot{x}) g \tag{5}$$

with

$$P_a = P[1 + \mu sgn(x) tg\alpha] \tag{6}$$

where μ and μ_F denote the dynamic friction coefficients for solid and viscous-like friction forces, respectively.

Collisions between the granular block and the trough are generally inelastic. The velocity of the granular block after the collision is given by

$$\underset{i}{\dot{x}} = \varepsilon_t \dot{x}(t_i) \tag{7}$$

$$\underset{i}{\dot{y}} = -\varepsilon_n \dot{y}(t_i) \tag{8}$$

where the subscript i reflects the corresponding values right at the impact. The restitution coefficients ε_t and ε_n can take arbitrary values from 0 to 1.

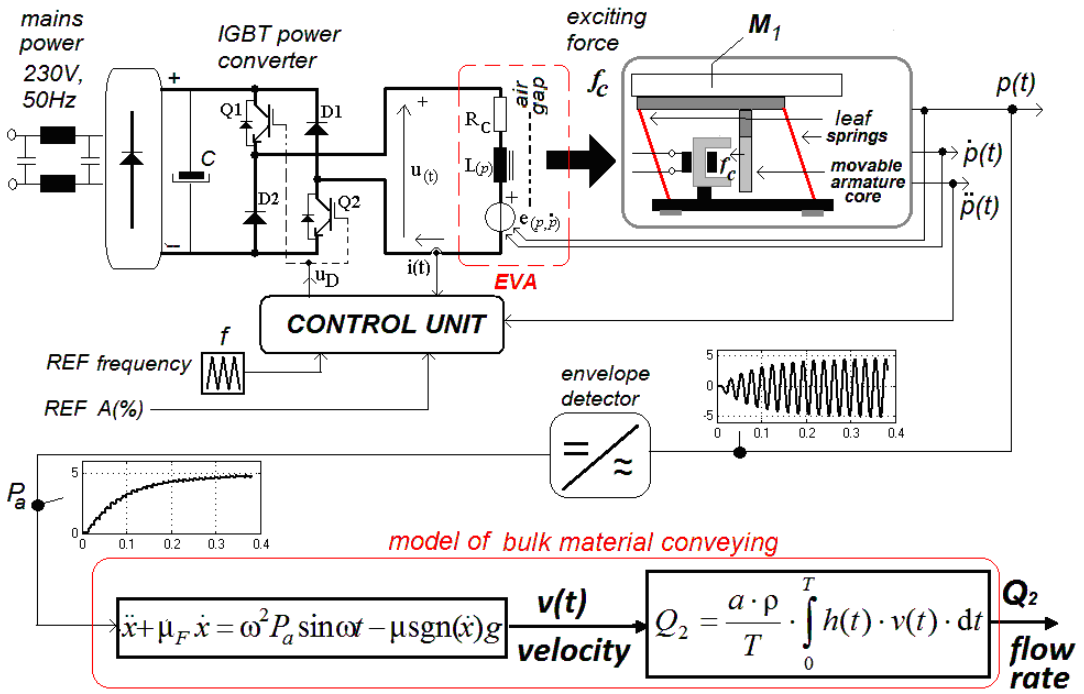

Fig. 1. Block diagram of the mathematical model of EVF

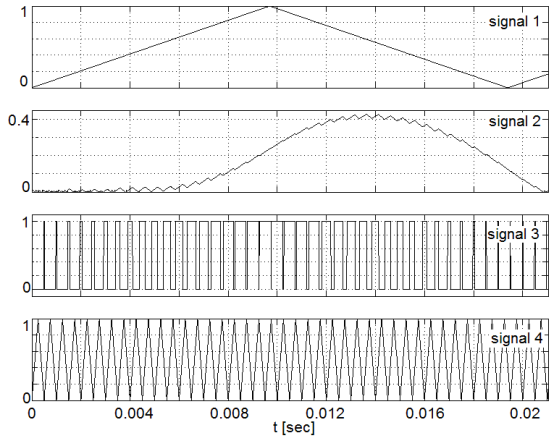

Fig. 2. Waveforms of the characteristic control signal of the switching power converter

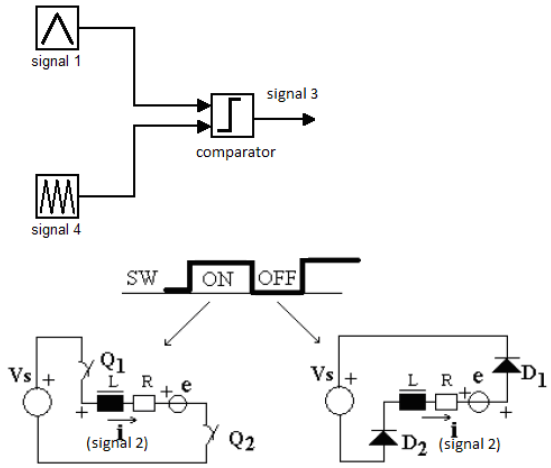

Fig. 3. Schematic diagram of asymmetrical half-bridge switching power converters and PWM pulse generation

The free flight phase starts at the lift-off time t_l determined by $\omega^2 Ptg\alpha \sin \omega t_l - g = 0$ and the equations of motion in the co-moving frame are then given by

$$\begin{aligned} m\,\ddot{x} &= m\omega^2 P \sin \omega t \\ m\,\ddot{y} &= m\omega^2 Ptg\alpha \sin \omega t - mg \end{aligned} \tag{9}$$

Calculation of material flow through the vibrating trough is done based on the velocity of the bulk material via the vibrating trough $v\,(t) = \dot{x}$.

For the purpose of modeling of the movement of material from the inlet hopper to the vibrating trough here are used the following symbols: Q_1 – the flow of material from the inlet hopper, adjusted using a shutter; *v(t)* – velocity of

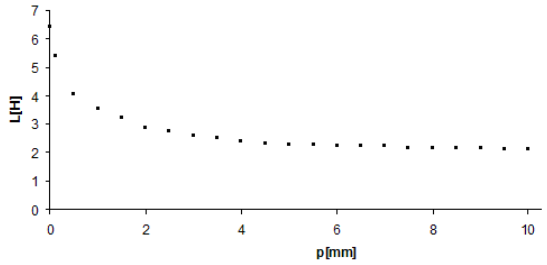

Fig. 4. The dependence of the inductance coil of the air-gap width

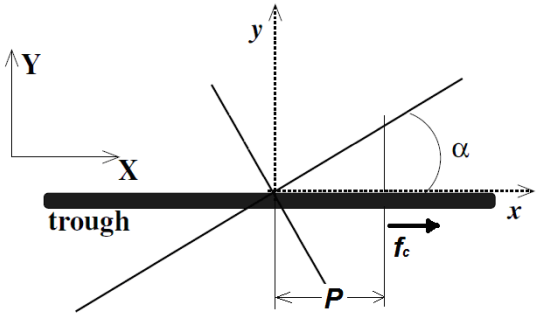

Fig. 5. Principal diagram of the linear vibratory conveyor including its external driving

the bulk material via the vibrating trough; *a* – trough width; *h(t)* – height level of the material in the trough directly below the shutter; *H* – maximum height level of the material in the trough directly below the shutter; ρ – density of the bulk material; *T* – Period of mechanical oscillation; *S* – cross-sectional area of the shutter.

The maximum mass of material that can come out of the inlet hopper during one period of mechanical oscillation is:

$$M_1 = Q_1 \cdot T \tag{10}$$

The velocity of material from the hopper is given as:

$$v_1 = \frac{Q_1}{S \cdot \rho} \tag{11}$$

The flow of material via the vibrating trough is given by the equation:

$$Q_2 = \frac{a \cdot \rho}{T} \cdot \int_0^T h(t) \cdot v(t) \cdot \mathrm{d}t \tag{12}$$

The actual value of height level of the material in the vibrating trough, directly below the shutter, is given by the following relation:

$$h\left(t\right) = \begin{cases} H, & for \quad v\left(t\right) \leq v_{cr} \\ \frac{M_1}{a \cdot \rho \cdot \int_0^T v(t) \cdot \mathrm{d}t}, & for \quad v\left(t\right) > v_{cr} \end{cases} \tag{13}$$

where v_{cr} represents the minimum value of $v\left(t\right)$ for which the condition $Q_2 = Q_1$is fulfilled.

Equation (13) shows that the level of the material, directly below the shutter, has a constant value while the condition $v\left(t\right) \leq v_{cr}$ is fulfilled. The increase in velocity of the material in the trough over the critical value v_{cr} causes a decrease of level of the material directly below the shutter. This decrease in the level of the material is due to the limitations of the material flow through the vibrating trough. The maximum possible value of the flow of material through the vibrating trough is Q_1.

It is assumed that the flow of material is the same at the beginning and at the end of the vibrating trough. By observation it was determined that the trough level of the material is decreasing linearly along the trough, for $v(t) \leq v_{cr}$. Based on this assumption, it is ignored what happens to the material along the vibrating trough, and accordingly the flow of the material is determined to flow value which is directly below the shutter.

In the previous consideration, the bulk material was then observed as portion to be transported during one period of oscillation.

For $v\left(t\right) \leq v_{cr}$, the level of material, directly below the shutter, is constant and it is equal H. During one period of mechanical oscillation, the flow of bulk material from the hopper compensates the portion of material that is transported to the end of the vibrating trough. Based on other known values the flow of the material via the vibrating trough is calculated.

For $v\left(t\right) > v_{cr}$, the material moves under the shutter, but in that case the flow of material fills this space only to a certain level. In particular, this volume should be filled by material that comes from the hopper, i.e. material mass M_1. Height level of the material directly below the shutter is calculated according to (13). Based on these values, the average value of the material velocity and other known parameters is used to calculate the material flow.

The simulation model requires specific parameters for each type of bulk material and provides the possibility of investigation of the influence of external disturbances to the system.

3 SIMULATION RESULTS

This section presents the results obtained by the simulation model, based on the mathematical model of vibratory feeder loaded with transporting material presented in the previous section. The simulation model of EVF is created in Simulink/Matlab. Block diagram of the simulation model of EVF is identical to the model presented in Fig. 1.

The basic mechanical parameters of the simulation are: m_{k0} - mass of the moving part of the vibratory conveyor, k_e

- total stiffness of the elastic elements, and b_e - damping of the system. On the basis of these parameters the mechanical parameters of the system which appear in the model are calculated: static gain - $K_p = 1/k_e$ and damping factor $\xi = b_e/2m_{k0}\omega_0$. There are three case of stiffness of the elastic elements: 215.379925 N/mm, 138.89565 N/mm and 97.5220135 N/mm. These springs correspond to the following triplets (f_{mr}, K_p, ξ): (64.2 Hz, 0.00464 mm/N, 0.027), (51.5 Hz, 0.00721 mm/N, 0.01674) and (43.2 Hz, 0.01025 mm/N, 0.04), respectively. The real electrical parameters of the simulation are: $R_c = 81.5\Omega$ - active resistance of EVA coil, $L_0 = 2.72H$ - inductance of EVA coil, and $V_s = 400V$ - power supply voltage. The real value of the mechanical parameters of the simulation are:$p_0 = 2.5mm$,$d = 0.5mm$,$\rho = 800Kg/m^3$,$a = 5cm$, $Q_1 = 0.058Kg/\sec$ and $H = 16mm$.

Figures 6-8 show the dependence of the bulk material flow and average value of the EVA current in depend of the EVA current frequency (f). Simulations were performed for the following values off_{mr}: 64.2 Hz, 51.5 Hz and 43.2 Hz. Mathematical model refers to EVF with an excitation frequency equal to the mechanical resonant frequency. For this reason, flow characteristics are valid only for excitation frequencies that are near the resonant frequency.

The maximum bulk material flow rate is achieved, if the EVA current frequency is equal to f_{mr}. For other values of the EVA current frequency, there is a significant increase of the bulk material flow rate only if$f = k^{-1}f_{mr}$, for$k \in N$.

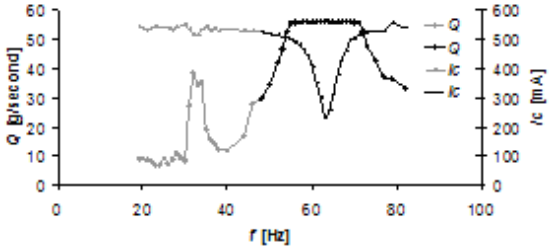

Fig. 6. Flow characteristic depending on frequency and average value of the EVA current, fmr = 64.2 Hz, A = 70 %, simulation

Figures 9-11 show some of typical time diagrams of displacement of the trough and the EVA current, for the following values of mechanical resonant frequency f_{mr}: 43.2 Hz, 51.5 Hz and 64.2 Hz, respectively. The channel (1) shows the displacement$p\,(t)$. The channel (2) shows the coil current $i_c\,(t)$.

4 DESCRIPTION OF EXPERIMENTAL SETUP

The vibratory feeder has been designed in order to determine correlation of bulk material flow with respect to

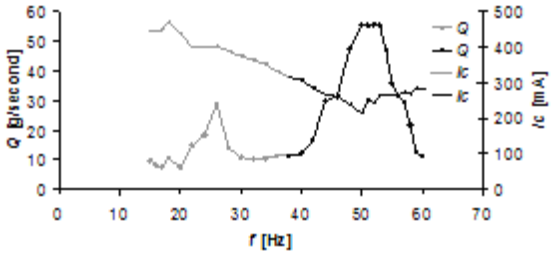

Fig. 7. Flow characteristic depending on frequency and average value of the EVA current , fmr = 51.5 Hz, A = 50 %, simulation

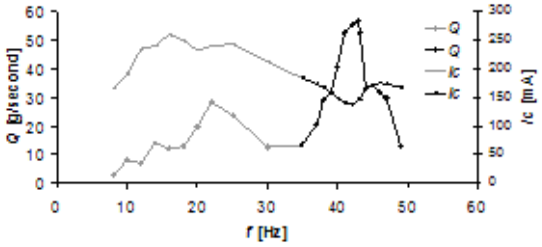

Fig. 8. Flow characteristic depending on frequency and average value of the EVA current, f_{mr} = 43.2 Hz, A = 30 %, simulation

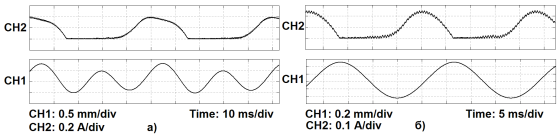

Fig. 9. Time diagram of displacement (CH1) and the EVA current (CH2), f_{mr} = 43.2 Hz. (a)- f = 20 Hz, (b)- f = 43.2 Hz

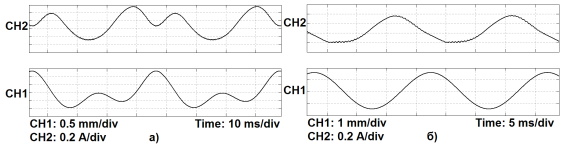

Fig. 10. Time diagram of displacement (CH1) and the EVA current (CH2), f_{mr} = 51.5 Hz. (a)- f = 24 Hz, (b)- f = 51 Hz.

oscillation frequency and average value of the excitation coil current. The main objective of this experimental research is experimental verification of the adopted model and it also defines the parameters that enable the selection of energy-efficient operating point of the EVF.

The block diagram of this experimental setup is shown on Fig. 12.

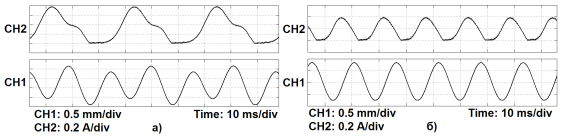

Fig. 11. Time diagram of displacement (CH1) and the EVA current (CH2), f_{mr} = 64.2 Hz. (a)- f = 32 Hz, (b)- f = 64 Hz.

Table 1. The ratio of parameter A [%] and average value of the EVA coil current

fmr = 43.2 Hz		**fmr = 51.5 Hz**		**fmr = 64.2 Hz**	
À[%]	Ic[mA]	À[%]	Ic[mA]	À [%]	Ic[mA]
10	90	10	80	10	70
20	120	20	110	30	120
30	150	30	140	50	170
40	190	40	170	70	230
50	225	50	210	90	290

This system has the following elements: (1)-digital control unit (DCU), (2)-inlet hopper, (3)- shutter to adjust the mass flow of material from the inlet hopper (4)- vibrating trough, (5)-acceleration sensor mounted on the base plate of the vibrating trough (6)- EVA, (7)- displacement sensor of the trough, (8)-laminated composite springs, (9)-force sensor of the weighed material, (10)- damping elastic elements, (11)- base of EVF, (12)- current sensor and (13)-oscilloscope for the tests.

The digital control unit (DCU) uses signals from sensors for monitoring of amplitude and frequency of oscillation. In addition to this, main function of DCU is to control the power converter operation, by using reference values of an excitation frequency and excitation power. Data entry is performed via integrated keyboard and overall operation is monitored by using a liquid-crystal-display (LCD). Excitation power ($A[\%]$) is a parameter that represents the percentage of maximal power which could be forwarded to the EVA coil and it is proportional to the average value of the EVA excitation current ($I_c[mA]$).

The ratio of parameter $A[\%]$ and average value of the EVA coil current ($I_c[mA]$) is shown in Table 1, for three characteristic values of mechanical resonant frequency of the EVF (f_{mr}).

The ratio of parameter A [%] and the amplitude of oscillations P[mm] is shown in Fig. 13, for three characteristic values of the mechanical resonant frequency.

The base of EVF is made from solid block, in order to support the transferring of vibrations from actuator to the trough. Those vibrations induce the flow of granular material. Transfer of vibrations from EVF to the environment is reduced using damping-elastic elements. The construction allows an elastic foundation of the vibrating trough to the base of EVF. The proposed construction permits montage of the hopper above of vibrating trough. Displacement sensor is externally mounted near the armature of EVA, as shown in Fig. 1.

The carrier of composite springs represents a supporting point for inductor of EVA.

The springs are made of fiberglass. Within the setup kit there are four pairs of springs, which have different thicknesses. The combination of these springs is used to adjust the coefficient of elasticity of the equivalent spring in order to adjust the mechanical resonant frequency of EVF. These elastic elements of EVF are subject to very high dynamic strain and they are the most critical element of the device from the standpoint of reliability [14].

The inlet hopper makes possible a gravimetric flow of an input granular material. The flow of the material from the hopper can be adjusted using a shutter. Diameter of the shutter is 3 ". The hopper volume is about 2 liters.

The acceleration sensor (P/N 123-215) is attached to the base of vibrating trough.

The displacement sensor (TURCK NI10-M18-LiU) is mechanically fastened to the base. The signal at the output of this sensor is proportional of relatively displacement between the armature EVA and base of EVF (p), as shown in Figure 12. The maximum displacement of the trough is mechanically limited to value of 3 mm.

The average value of the coil current is measured by the digital multimeter. The current sensor with optical isolation is used for monitoring actual EVA current, and additionally using the conventional digital storage oscilloscope (GDS-1052-U).

5 EXPERIMENTAL RESULTS

Before the start of the recording of the characteristics, frequency excitation is equal to the mechanical resonance and the value of the parameter $A[\%]$ is increased until the flow of material from the channel exceeds the inflow of material from the hopper. When recording the flow characteristics, value of the parameter $A[\%]$ has not been changed. Since the lab kit has three different pairs of spring elasticity, it is possible to record the flow characteristics of three cases of mechanical resonance. As these frequencies cover the area of application of the most common feeders, based on the obtained characteristics it is possible to perform general conclusions relating to this type of feeders.

Figures 14-19 graphically represent experimental results. Figures 14-16 show the dependence of the flow of bulk material and average value of the EVA current from the frequency of the EVA current pulses, for the following values of f_{mr}: 64.2 Hz, 51.5 Hz and 43.2 Hz, respectively.

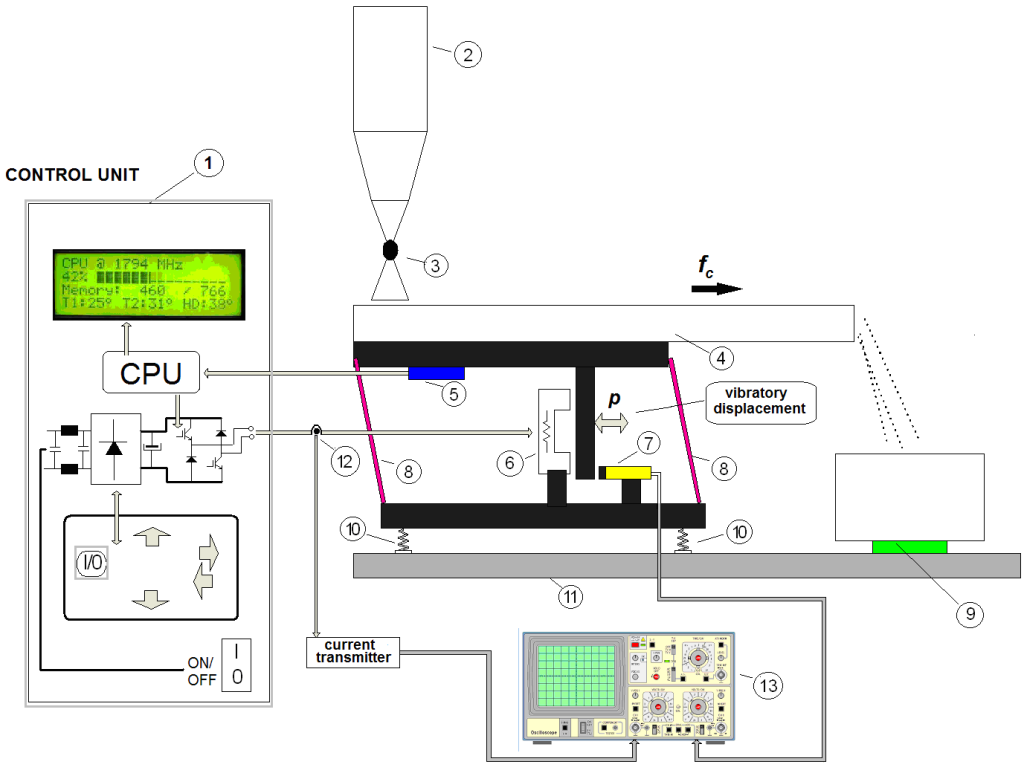

Fig. 12. Block diagram of the experimental setup

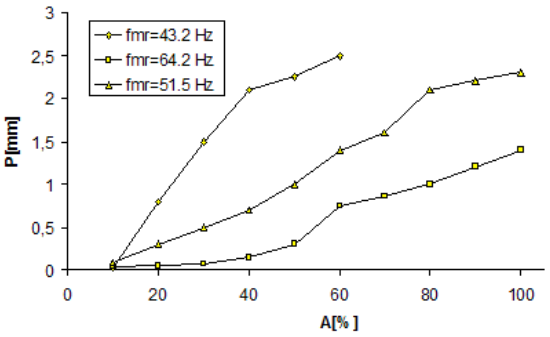

Fig. 13. The ratio of parameter A [%] and the amplitude of oscillations P[mm]

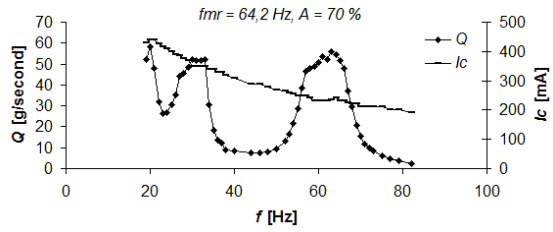

Fig. 14. Flow characteristic depending on frequency and average value of the EVA current, f_{mr} = 64.2 Hz

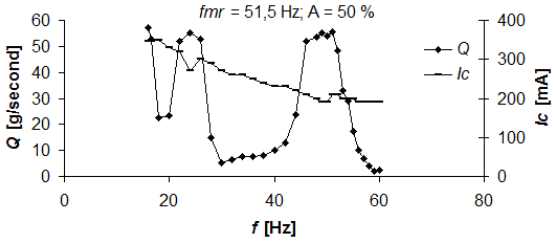

Fig. 15. Flow characteristic depending on frequency and average value of the EVA current, f_{mr} = 51.5 Hz

Within the time interval between two current pulses, feeder naturally oscillates. These oscillations are damped and their frequency represents the mechanical resonant frequency of the feeder. The largest material flow is achieved for frequency of the current pulses which is equal to the mechanical resonant frequency of the feeder or a whole number of times less than the resonant frequency. For other values of frequency of the current pulses, material flow is significantly lower as a result of the energy consumption of electrical impulses to overcome the energy that is stored in the springs of the feeder. It is concluded that, in order to achieve maximum material flow, frequency current pulses

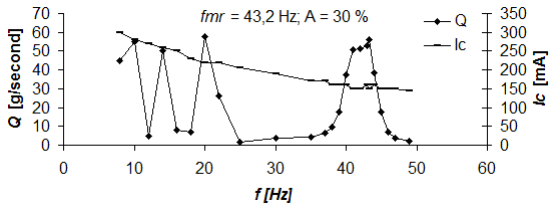

Fig. 16. Flow characteristic depending on frequency and average value of the EVA current, f_{mr} = 43.2 Hz

should be adjusted to excite the natural oscillations of the feeder.

Figures 17-19 show some of typical time diagrams of displacement of the trough and the EVA current, for the following values of f_{mr}: 43.2 Hz, 51.5 Hz and 64.2 Hz, respectively. On the channel (1) shows the signal obtained from the movement sensor. The channel (2) shows the signal obtained from the current sensor.

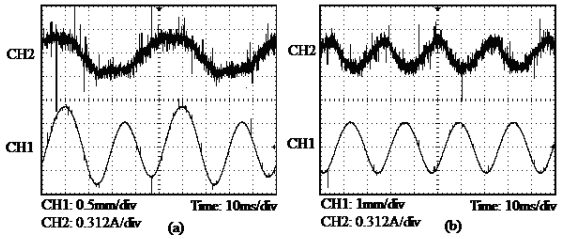

Fig. 17. Time diagram of displacement (CH1) and the EVA current (CH2), f_{mr} = 43.2 Hz. (a)- f = 20 Hz, (b)- f = 43.2 Hz

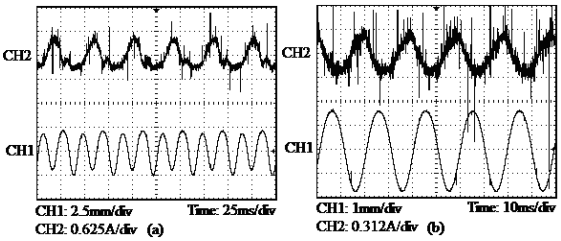

Fig. 18. Time diagram of displacement (CH1) and the EVA current (CH2), f_{mr} = 51.5 Hz. (a)- f = 24 Hz, (b)- f = 51 Hz.

It was observed that with an increase in the frequency of the current pulses leads to reduction in the average value of current and to a reduction of displacement of the vibrating trough in the horizontal plane.

The excitation of EVA with current pulses whose frequency is an integer times lower than the resonant frequency of the feeder can provide feed rate as when the EVA is energized by current pulses whose frequency is equal to

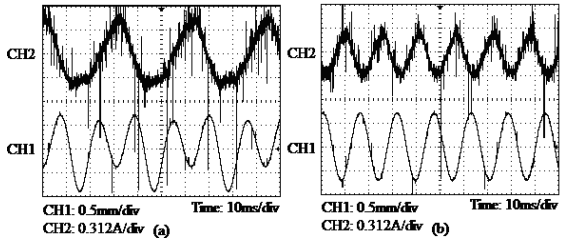

Fig. 19. Time diagram of displacement (CH1) and the EVA current (CH2), f_{mr} = 64.2 Hz. (a)- f = 32 Hz, (b)- f = 64 Hz.

the mechanical resonant frequency of the feeder, but with a higher energy consumption and with greater mechanical stress of springs.

If the EVA is energized with current pulses whose frequency is equal to the mechanical resonant frequency of the feeder, the maximum material flow is obtained with minimal energy consumption and minimal mechanical stress of springs (minimal displacement of the vibrating trough in the horizontal plane).

The above figures are obtained for excitation current pulses obtained by applying PWM voltage modulation, whereas the high-frequency noise in current is the consequence of PWM power converter operation.

6 COMPARISONS OF SIMULATION AND EXPERIMENTAL RESULTS

The obtained simulation and experimental results confirm that the model adopted by the EVF is acceptable if the EVA is excited with current pulses whose frequency close to the mechanical resonance of the EVF.

Comparing Figs. 6-8 to Figs. 14-16, respectively, concludes that the approximate model of the EVF has a satisfactory response for the EVA current frequency above the first sub-resonant frequency. Considering that the modeling was carried out for a system with EVA energized with current pulses whose frequency is equal to the mechanical resonant frequency of the feeder, there are certain differences between simulation and experimental results for sub-resonant frequency excitation. Bearing in mind that the scope of the excitation frequency, which is used in practice, is near the resonant frequency, these differences are acceptable, and do not affect the resonance-frequency operation of the feeder.

Flow characteristics show saturation for increasing flows of bulk material, and for excitation frequencies near to the mechanical resonance frequency. This saturation is due to relatively large value of the parameter $A\,[\%]$ i.e. relatively large average value of the EVA current, due to

which the bulk material flow reaches its maximum value equal to the flow of material from the inlet hopper.

Provided that critical velocities $v_{cr}$are not reached two EVF devices with different mechanical resonant frequencies whose excitation frequency are equal to their mechanical resonances, will achieve the same flow rate if EVF with lower mechanical resonant frequency achieves greater displacement of the trough. In the case when critical velocities are reached further increasing the value of the parameter $A[\%]$ causes an increase in the mean value of the excitation currents, and thus the increase in displacement of troughs, but there is no increase in flow rate. The mean value of the excitation current at which a critical velocity of material in the vibrating trough is reached represents a limit current value at which the EVF goes to flow saturation. Figure 18 shows a timing diagram of the EVF in which the excitation current is greater than the limit value, so the displacement is larger than in Fig. 17, which represents the time diagram of the EVF with lower mechanical resonant frequency. This may be considered as an additional contribution, because the critical velocity of material in the vibrating trough and the limit value of excitation current is not considered in the cited literature. Defining these values enables the selection of energy-efficient operating point of the EVF.

7 CONCLUSIONS

This paper presents the results of an experimental research of the bulk material flow rate and average value of excitation coil current of electromagnetic vibratory feeder in dependence on the frequency of the excitation coil current of EVF. In addition to modeling of the EVF, the main contribution of this paper is implementation of flow control algorithm of bulk material on EVF, experimental verification of the adopted model and defining of parameters that enable the selection of energy-efficient operating point of the EVF.

In comparison to the cited literature, which considers only certain subsystems of the EVF, this paper has experimentally verified the proposed model of the entire resonant EVF in Simulink/Matlab and defines the critical velocity of the material in the vibrating trough and the excitation current limit value. These defined parameters enable the selection of energy-efficient operating point of the EVF. In other words, in energy-efficient operating point of the EVF excitation frequency is equal to the mechanical resonant frequency of the EVF and velocity of the material through the vibrating trough is equal to critical velocityv_{cr}. Finding this point is important for the use the EVF in systems with feedback.

It has been experimentally confirmed that the bulk material flow rate has its maximum value as far as excitation frequency is equal to the EVF mechanical resonant frequencyf_{mr}. It is the global maximum of the bulk material flow rate. Local maximum of the bulk material flow rate is achieved if coil current frequency is integer number of times smaller then the EVF mechanical resonant frequencyf_{mr} (sub-resonant frequency). This is due to the tendency of the system to oscillate on the resonant frequency. For certain bulk material flow rate, average value of excitation coil current of EVF has minimal value when excitation frequency is equal to mechanical resonant frequency. In this case the EVF is the most energy efficient.

Most of the EVF is designed for continuous operation over relatively long time intervals. In the case of EVF with lower mechanical resonance, to achieve the maximum flow of materials, it is necessary to provide a larger shift of the vibrating trough in a horizontal plane. In this way, the springs are exposed to high mechanical stresses, so selection of a material for springs is of particular importance. Springs used in this study are made of fiberglass and they have given satisfactory results.

Since the adopted simulation model is designed based on the mathematical model of the EVF whose excitation frequency is equal to the mechanical resonant frequency of the EVF, the obtained results represent experimental verification of the adopted simulation model. Adopted model of the EVF has a satisfactory response for the EVA current frequency above the first sub-resonant frequency. This frequency area is determined as area of validity of the adopted simulation model.

Additionally increasing of the flow rate should be achieved by generating electrical impulses in the moments of passing the trough by the equilibrium position, in other words by introduction a feedback per phase of the EVA current pulses. In this way, the input energy would not be consumed to overcome the accumulated energy in the springs.

In modern EVF finding the resonant frequency is done by changing frequency excitation from the smallest to the largest value in a given range and measuring the displacement of the vibrating trough. The algorithm is designed so that the search scope stops when it finds the first maximum displacement. This research has shown that the maximum displacement can be local, which corresponds to a sub-resonant frequency of the excitation, or global, which corresponds to the resonant frequency of the excitation. Since the mechanical resonance depends on the coefficient of elasticity of the elastic elements and of the total weight of cargo that relies on them, algorithms for finding the resonant frequency should be designed such that it does not include the sub-resonant frequency. If the coefficient of elasticity of the springs and the expected weight of the cargo are known, this requirement is not difficult to achieve.

ACKNOWLEDGMENT

The authors gratefully acknowledge the constructive comments and valuable suggestions of anonymous reviewers. This investigation has been carried out with the financial support of the Serbian Ministry of Education, Science and Technological development within the project No: TR33022.

REFERENCES

[1] A.J. Pullan, M.L. Buist, L.K. Cheng, *Mathematically Modelling the Electrical Activity of the Heart - From Cell to Body Surface and Back Again*, World Scientific, 2005.

[2] I.F.Goncharevich, K.V.Frolov, and E.I.Rivin, "Theory of vibratory technology", Hemisphere Publishing Corporation, placeStateNew York, 1990.

[3] T. Dyr and P. Wodzinski, ,"Model particle velocity on a vibrating surface," Physicochemical Problems of Mineral Processing, Vol. 36, pp. 147-157, May 2002.

[4] L.Han and S.K.Tso, "Mechatronic design of a flexible vibratory feeding system", Proceedings of the I MECH-E-Part B Journal of Engineering Manufacture, Vol.217, No.6, June 2003, pp.837- 842.

[5] E.M. Sloot and N.P Kruyt, "Theoretical and experimental study of the transport of granular materials by inclined vibratory conveyors", Powder Technology, Vol.87, No3, pp.203-210, 1996.

[6] M.A. Parameswaran and S.Ganapahy, "Vibratory Conveying-Analysis and Design: A Review", Mechanism and Machine Theory, Vol.14, No.2, pp. 89-97, April 1979.

[7] D.McGlinchey, "Vibratory Conveying Under Extreme Conditions: An Experimental Study", Advanced in Dry Processing 2002, Powder/Bulk Solids, pp.63-67, November 2001

[8] T. Doi, K. Yoshida, Y. Tamai, K. Kono, K. Naito, and T. Ono, "Modelling and feedback control for vibratory feeder of electromagnetic type," Journal of Robotics and Mechatronics, Vol. 11, No. 5, pp. 563-572, Jun. 1999.

[9] J. Sokolov, V. I. Babitsky, and N. A. Halliwell, "Autoresonant vibro-impact system with electromagnetic excitation," Journal of Sound and Vibration, No. 308, pp. 375-391, 2007.

[10] Z. Despotovic and Z. Stojiljkovic, "Power converter control circuits for two-mass vibratory conveying system with electromagnetic drive: Simulations and experimental results," IEEE Trans. Ind. Electron., Vol. 54, No. 1, pp.453-466, Feb. 2007.

[11] A.I.Ribic and Z.Despotovic," High-Performance Feedback Control of Electromagnetic Vibratory Feeder", IEEE Transaction on Industrial Electronics, Vol.57, Issue :9, Aug. 2010,pp.3087-3094.

[12] V.I.Babitsky, "Autoresonant Mechatronics Systems", Mechatronics 5 (1995), pp. 483-495.

[13] Ž.V. Despotović , A. I. Ribić, V.Sinik , "Power Current Control of a Resonant Vibratory Conveyor Having Electromagnetic Drive", Journal of Power Electronics, Vol.12, No4, July 2012.

[14] Complete Guide to Vibratory Feeders and Conveyors, "How To Choose and Use Vibratory Feeders and Conveyors" , ERIEZ CityplaceMagnetics,, StatePennsylvania, country-regionUSA, pp.3-13, 2003

[15] Milica M. Vujović, Željko V. Despotović, "Dynamic Stress Distribution in Composite Leaf Springs for Electromagnetic Vibratory Feeder ", MECHEDU, 2015.

[16] Spring manual for Vibratory Conveyors and Feeder, "The use of Composite Leaf Springs in Vibrating Machinery" HEATHCOTE INDUS-TRIAL PLASTICS, Vol. I, pp.1-16, CityplaceNewcastle- under-Lyme, 2004, www.heathcotes.com

[17] Z.V.Despotovic, M.Lecic, M.Jovic, A.Djuric, "Vibration control of resonant vibratory feeder with electromagnetic excitation," Journal FME Transactions, Vol.42, No.4, pp281-289, 2014.

[18] Hamid El hor & Stefan J. Linz, „Model for transport of granular matter on an annular vibratory conveyor", Journal of Statistical of Mechanics: Theory and Experiment, (2005) L02005.

[19] Grzegorz M. Krolczyk, Jolanta B. Krolczyk, Stanislaw Legutko, Anica Hunjet, "Effect of the disk processing tehnology on the vibration level of the chipper during operations process", Tehnicki vjesnik – Technical gazette, 21, 2 (2014), pp. 447-450).

P. J. Mišljen was born in Zadar, Croatia, in 1980. He received the B.Sc and M.Sc. degree from the Logistic Depatment, Military Academy, University of Defense, Belgrade, Serbia, in 2004, and became engineer of electronics, specialty missile systems. In the period from 2004 to 2010 he worked as a supervisor at the facility to maintain electronic resources and missile systems. In 2011 he enrolled in doctoral studies at the Faculty of Engineering, University of Kragujevac, Centre for Applied Automatic Control. His research interests include the fields of industrial electronics and mechatronics.

Ž. V. Despotović was born in Prijepolje, Serbia. He received the B.Sc., M.Sc., and Ph.D. degrees from the Chair of Power Converters and Drives, School of Electrical Engineering, University of Belgrade, Belgrade, Serbia, in 1990, 2003, and 2007, respectively. He has been with the Department of Robotics and Mechatronics- Mihajlo Pupin Institute, University of Belgrade, since 1991. His research interests include the fields of power electronics, industrial electronics, mechatronics and vibration control. His currently positions in Mihajlo Pupin Institute are: Associate Research Professor and Head R&D Engineer of Power Electronics. It has a Graduate Engineer's Licenses: Responsible Designer of Electrical Drive Control - automatic, measuring and regulation and Responsible Designer of Low and Medium Voltage Power System, Serbian Chamber of Engineers. He is professor at the High School of Professional Studies in Electrical Engineering and Computer Science - Belgrade, Serbia, since February 2010. He is professor at PhD academic studies on the School of Electrical Engineering, University of Belgrade-Chair of Power Converters and Drives (teaching courses: Power Converter, Control of Power Converter), since 2014. He is IEEE senior member, since 2015.

M. S. Matijević received the Dipl.Ing., M.Sc. and Ph.D. degrees at University of Kragujevac. He was the best graduated student at University of Kragujevac, then, TA/RA, Docent, Associate Professor, respectively, and since 2012, he has been an Full Professor with the Faculty of Engineering at University of Kragujevac (FEUniKG), teaching courses in automatic control. In school year 2010/11 he was a Fulbright Scholar at MIT. On May 30, 2016 he elected for the member of Serbian Scientific Society. He is Head of the Centre for Applied Automatic Control at FEUniKG. His scientific interests are in the areas of system modeling and identification, applications and design of computer controlled systems.

AUTHORS' ADDRESSES

Petar Mišljen, Dipl.Ing.
Prof. Milan Matijević, Ph.D.
University of Kragujevac,
Faculty of Engineering,
Centre for Applied Automatic Control,
6, Sestre Janjic Str, 34000 Kragujevac, Serbia
e-mail: pmisljen@kg.ac.rs, matijevic@kg.ac.rs

Željko Despotović, Ph.D. University of Belgrade, Mihajlo Pupin Institute, Department of Robotics and Mechatronics 15, Volgina Str, 11000 Belgrade, Serbia e-mail: zeljko.despotovic@pupin.rs

Received: 2016-04-22
Accepted: 2017-02-13